Novel Passive Controller Design for Enhancing Boost Converter Stability in DC Microgrid Applications

Fulong Li, *Member, IEEE,* Zhengyu Lin, *Senior Member, IEEE,*

Abstract—Boost converters have Non-Minimum Phase (NMP) characteristics, which makes the stable closed loop control design difficult. Based on the passive theory, this paper proposes to add a feed-forward loop in the conventional double loop closed loop to compensate the NMP effect. Therefore, the potential instability caused by NMP can be avoided. Such compensation is especially useful for DC microgrids applications where boost converters are widely used as interface converters. Two types of feed-forward gain are discussed and compared. The gain of K with high-pass filter is used eventually for integrating with conventional droop control because it does not change low frequency quiescent operation point. The stability of the proposed controller is analysed through loop gain on s-plane. Besides, how the output impedance of converter is shaped by the passive controller is analysed. The experimental results validate the effectiveness of the proposed passive controller.

Index Terms—boost converter, DC microgrid, non-minimum phase, passivity, stability.

I. INTRODUCTION

DC microgrids have been a popular research topic recently due to the advantages of integrating renewable energy sources and energy storage over conventional AC grids, such as higher efficiency, controllability and flexibility [1].

A DC microgrid usually contains distributed power generations, such as photovoltaic (PV) and wind energy, energy storage and loads. Boost converters are widely used in DC microgrids to connect low voltage DC energy sources to the high voltage DC bus. However, when a boost converter is operated as continuous conduction mode, it exhibits Right Half Plane (RHP) zero or NMP in the control to output voltage transfer function. The NMP effect of boost converters has the potential to threat converter stability in some cases [2]. Therefore, when a boost converter is connected to a DC microgrid, it may cause the DC system instability. The instability factors in a DC microgrid can be inspected from both source and load sides [3]. From the load side, the instability is commonly caused by constant power loads (CPLs), such as point of load converters. From the source side, the instability could be caused by a single converter or converters in parallel. The instability of a boost converter is mainly caused by the improper control design. The instability of converters in parallel can be found in the droop control based DC systems [4]. The NMP issue is categorized into single converter instability.

Different techniques to eliminate the NMP effect of boost converters have been proposed in the last few decades, and they can be broadly categorized into two types, which are from power stages and from control strategies, respectively.

In term of power stages, a magnetic coupling method [5] is proposed. An additional output filter is added to the boost converter output terminal, and is coupled with the boost converter inductor. This method can be used to eliminate the NMP effect, however, the overall size of the converter is increased. Also, this method modifies the converter topology and makes it lack of generality to deal with NMP effect. An interleaved boost converter [6] is proposed to alleviate the NMP effect. Besides, an auxiliary current injection circuit for such interleaved boost converter is proposed in [7] for improving the dynamic response degraded by NMP effect. Furthermore, an interleaved boost converter integrated with magnetic coupling method proposed and studied in [8]. A tri-state boost converter is proposed in [9]. Additional power switches and diodes are added to the topology to create a free-wheeling path for the inductor current. The above methods need additional components in the power stage to eliminate the NMP effect, which increase the complexity of the converter modeling and controlling.

From the controller design perspective, single loop voltage control is normally considered in conventional boost converter control to eliminate NMP effect. A leading-edge modulation method is proposed in [10] and [11] to shift the boost converter's RHP zero into the Left Half Plane (LHP). Some dedicated conditions have to be applied, such as the equivalent series resistance (ESR) of the output capacitor must be higher than a certain value. This large ESR will cause high boost converter output voltage switching ripples. This method is also further developed in [12].

Without utilising the output capacitor ESR, an output redefinition control method [13] is proposed. An additional nonlinear term is added to compensate the original NMP system to a Minimum Phase (MP) or marginally MP system. Other nonlinear methods, such as a nonlinear passive control method is proposed in [14]. However, the nonlinear control design process introduces complexity and lacks generality.

An internal model control is proposed in [15]. This method modifies conventional voltage control loop and adds an internal feed-forward path to the control blocks. For a single loop voltage controller, the order of plant transfer function is not reduced, and the controller design is still complicated.

For DC microgrids applications, commonly applied control

methods for boost converters are more than just single loop voltage control [12]. Double loop control has the advantage of order reduction in the outer loop control plant. Therefore, it may simplify the controller design [16]. The NMP in voltage control plant transfer function of a boost converter contains second order terms, which makes the system difficult to control and the compensator structure complex. The double loop control is able to eliminate the second order denominator and simplify the outer loop control plant. This also simplifies the controller design. Unfortunately, the NMP still exists in the double loop controller, and could make the system unstable.

Passivity-based control (PBC) can be used for converter control via Lyapunov-based advanced control methods [17]–[20]. A storage function is usually required for such design. A nonlinear disturbance observer is designed for buck converter in [17] to deal with CPLs. For interconnected system, an adaptive interconnection and damping assignment (IDA) passivity-based controller (PBC) for boost converters with CPLs is proposed in [20] where a Hamiltonian function is used to represents the total energy stored in the dynamic system. Cucuzzella *et al.* [18], [19] proposes Krasovskii-type storage function to deal with the system with unknown ZIP (constant impedance 'Z', constant current 'I' and constant power 'P') loads. The advantage of those methods is that it can directly solve the nonlinear problems occurred in cascaded converters, such as CPLs. However, those methods normally introduce large calculations and complexity and rely on dedicated applications. Apart from those methods, passive control theory is also used to study the impedance of converter because impedance-based stability analysis [21] is widely used for the DC microgrid stability evaluation.

Based on passive control theory, the instability issue caused by boost converters could be solved through modifying the internal controllers to shape the converter's input/output impedance. An active damping method is proposed in [22] to overcome the problems of CPL, where a negative feed-forward path is introduced to add the converter damping for CPL. In [23], a passive controller is proposed to modify the input impedance of load side converter and a low damping input filters is considered in the sources. The proposed passivity-based stability criterion is a strict criterion compared with conventional impedance based stability criteria, such as Middlebrook criterion [24]. Passivity-based stability criterion is further developed for the source side in [3]. A voltage feed-forward control is used to shape the boost converter output impedance. However, the introduced voltage feed-forward control needs to know the parameters of the original double loop control design, otherwise the impedance passivity of entire frequency cannot be guaranteed.

Considering the stability issue of boost converters in DC microgrid applications, this paper proposes to add a feed-forward passive controller in the conventional double loop controller to compensate the NMP in the transfer function. The added-on passive controller does not change the design procedure and forms of the conventional controller. Compared with existing techniques, it has the following advantages:

1. It does not change or modify the topology or working states of original boost converter, so the additional device and loss may be avoided;

2. It does not rely on the output capacitor ESR as it aims to compensate the RHP zero through the passive feed-forward path, so the converter output voltage ripple can be small;

3. It does not require to know the original double loop control design, so the design and implementation is simple and reliable, which is suitable for DC microgrid applications;

4. Due to the fact that the proposed control is based on linear methods, it avoids the complicated calculation in nonlinear PBC-based methods.

The rest of this paper is organized as follows: Section II gives brief introduction of passive theory and theorems related to this work. Section III provides the models of boost converter and explains how the passive controller is designed and applied in the control blocks. Two types of passivation methods are proposed and discussed. Controller design and impedance analysis of the proposed controller are conducted in Section IV. The experimental validation of the proposed method is shown in Section V. Conclusions are given in Section VI.

II. BRIEF INTRODUCTION OF PASSIVE THEORY

Passive theory is a systematic theorem to discuss the system stability (includes linear and nonlinear systems) and has many sub-theorems for different propositions and definitions. In this section, the theorems relevant to the design and requirement of interface converters are introduced. The full passivity theorem and related proofs can be found in [25]. Passive theory discusses the stability from energy perspective: if a system tends to consume energy, then the system always tends to be stable. It can be illustrated as follows:

Consider a system with state variables $x \in R^n$, $u \in R^m$, if there exists a non-negative function $H(x)$ and $\varepsilon(t)$ such that,

$$\int_0^t u^T(\tau) y(\tau) d\tau = H(x(t)) - H(x(0)) + \varepsilon(t) \quad (1)$$

then the system is passive.

In above equation, $\int_0^t u^T(\tau) y(\tau) d\tau$ represents the energy supplied to the system, $H(x(t)) - H(x(0))$ is the stored energy and $\varepsilon(t)$ represents the dissipated energy.

This theory gives the passive requirement in the linear system where the concept of positive real transfer functions is introduced.

Definition: A transfer function $G(s)$ is said to be positive real if

1). $G(s)$ is analytic in $Re(s) > 0$;

2). $G(j\omega) + G^*(j\omega) \geq 0$ for any frequency ω that $j\omega$ is not a pole of $G(s)$.

Here, $G^*(j\omega)$ is the complex conjugate transpose of $G(j\omega)$.

Theorem: A linear system is said to be passive if and only if its transfer function $G(s)$ is positive real.

The above theorem forms an input-output version of the positive-real lemma in the frequency domain. For single input single output passive systems, the condition $G(j\omega) + G^*(j\omega) \geq 0$ reduces to $Re(G(j\omega)) \geq 0$, which means that the real part of their frequency response is always non-negative. In other word, the phase shift is always within $[-90^o, 90^o]$, and for strictly passive system within
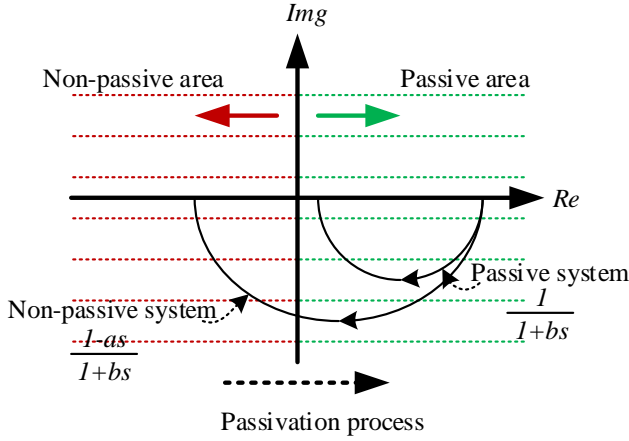
Fig. 1. Explanation of passive system on s-plane.

$(-90^o, 90^o)$. In real scenario, the controller has limited bandwidth. Besides, sampling components, such as current and voltage transducers, have limited bandwidth. Therefore, the phase shift actually can be bounded within the switching frequency; then the above boundary can be written as:

$$Re\left(G(j\omega)\right) \geq 0, \ \omega \in (0, \ 2\pi f_s) \tag{2}$$

where f_s is the switching frequency of a boost converter.

A passive system is always stable and easy to control. A good example is a simple first order system, and it can be described as follows:

$$G\left(s\right) = \frac{1 - a \cdot s}{1 + b \cdot s} \qquad (a, b \geqslant 0) \tag{3}$$

where a and b is the coefficient.

If $a = 0$, then this system is a passive system from the definition of passive theory. This system is always stable and its feedback control is also always stable [3].

If $a \neq 0$, then the numerator has a NMP and this system is not a passive system. This open loop system is stable, while its stability performance cannot be guaranteed when it has feedback control.

An effective way is to introduce feed-forward path to make such system passive. For a unit feed-forward control, this open loop system can be modified as:

$$G'\left(s\right) = 1 + \frac{1 - a \cdot s}{1 + b \cdot s} = \frac{2 + (b - a) \cdot s}{1 + b \cdot s} \tag{4}$$

For the above system, if $b - a \geqslant 0$, then the system is passive. In practical applications, a feed-forward gain is usually required as $b - a \geqslant 0$ can not always be achieved.

Therefore, the NMP effect of boost converter can then be rendered with passivation. The passivation here refers to make the plant passive and (strictly) positive real.

The passive area for general transfer functions in a s-plane is shown in Fig. 1 where if the function does not traverse the imaginary axis, the system is then passive.

III. PASSIVATION FOR BOOST CONVERTER

A. *Modelling and Analysis of Interface Converters*

The first step is to obtain the converter transfer functions. Modelling of boost converters with small signal analysis
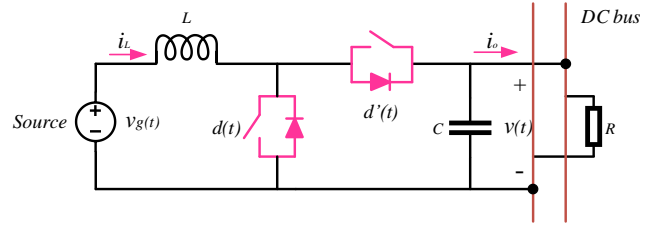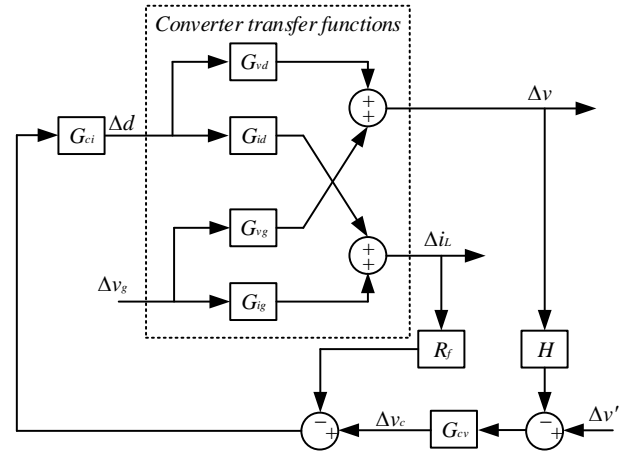

Fig. 2. Boost converter in a DC microgrid.

Fig. 3. Transfer function map of boost converter for assisting controller design.

has been done in previous literature [16]. For the analysis convenience and simplicity of models, the minor terms, such as inductor and capacitor equivalent parasitic resistances are ignored in this paper as they do not affect the design and function of the proposed controller.

A typical boost converter as an interface converter in a DC microgrid is shown in Fig. 2. Transfer functions for the boost converter are summarized below from equation (5) to equation (8).

$$G_{vd}\left(s\right) = \frac{V}{D'} \frac{1 - s\frac{L}{D'^2 R}}{den(s)} \tag{5}$$

$$G_{id}\left(s\right) = \frac{2V}{D'^2 R} \frac{1 + s\frac{RC}{2}}{den(s)} \tag{6}$$

$$G_{vg}\left(s\right) = \frac{1}{D'} \frac{1}{den(s)} \tag{7}$$

$$G_{ig}\left(s\right) = \frac{1}{D'^2 R} \frac{1 + sRC}{den(s)} \tag{8}$$

where $den\left(s\right) = 1 + s\frac{L}{D'^2 R} + s^2 \frac{LC}{D'^2}$.

The transfer functions are assembled and displayed in Fig. 3 for the convenience of controller design.

The inner loop transfer function G_{id} is shown in equation (6). The inner loop control plant has a minimum phase numerator and a second-order denominator with infinite amplitude gain. All the passive components in the circuit are always larger than zero and the duty cycle D is always between (0,1),
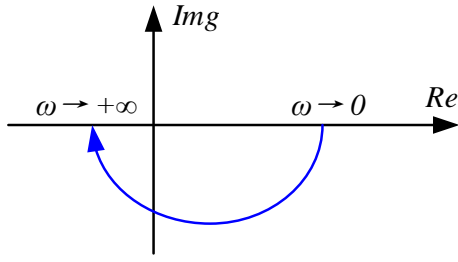
Fig. 4. Outer loop control plant of boost converter on s-plane.

Fig. 5. Control blocks of feed-forward compensation for outer loop plant.

which mean that the inner loop G_{id} has no intersection with negative part of real axis on s-plane. Thus, the inner loop is always stable.

The outer loop plant cannot be visibly shown from state equations, yet it can be obtained from the transfer function map [16], and it can be written as:

$$G_{vc} \approx \frac{1}{R_f} \cdot \frac{G_{vd}}{G_{id}} = \frac{D'R}{2R_f} \cdot \frac{1 - s\frac{L}{D'^2 R}}{1 + s\frac{RC}{2}} \qquad (9)$$

It can be seen that the second-order denominator is eliminated, and the order of plant is reduced. Normally, the controller can be designed according to the control plant. However, the numerator still contains the NMP, and it makes the outer plant have negative value over some frequency on s-plane, which does not satisfy the positive real requirement. This may be the potential threat to the system stability. The plant G_{vc} is drawn on s-plane in Fig. 4.

To analyze how system components affect the system dynamics, for the calculation and reading convenience, let:

$$\alpha = \frac{D'R}{2R_f}, \quad \beta = \frac{L}{D'^2 R}, \quad \gamma = \frac{RC}{2} \qquad (10)$$

Then, the equation (9) becomes:

$$G_{vc} \approx \alpha \frac{1 - s\beta}{1 + s\gamma} \qquad (11)$$

The dynamics over frequency domain can be analyzed by substituting $j\omega$ for s,

$$G_{vc} \approx \alpha \frac{1 - s\beta}{1 + s\gamma} = \alpha \frac{(1 - \omega^2 \beta\gamma) - (\beta+\gamma)\omega j}{1 + \omega^2 \gamma^2} \qquad (12)$$

In (12), the denominator is always positive, but the real part $1 - \omega^2 \beta\gamma$ can be negative when ω is large. Therefore, at the low frequency and high frequency, the asymptotic value of G_{vc} is shown below.

$$\omega \to 0, \quad G_{vc} \to \alpha = \frac{D'R}{2R_f} \qquad (13)$$

$$\omega \to +\infty, \quad G_{vc} \to -\frac{\alpha\beta}{\gamma} = \frac{-L}{R_f D'RC} \qquad (14)$$

Equation (14) has negative value, and increasing the value of capacitor C and decreasing the load (increasing the value of R) can make the total value move closer to the imaginary axis. Therefore, one intuitive conclusion can be made is that increasing the capacitor or decreasing the load tend to make the system more stable in thi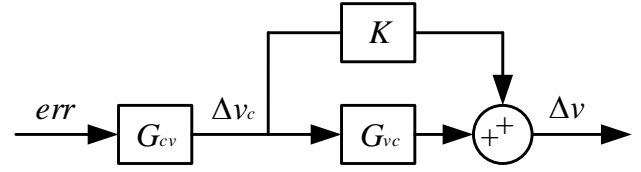s case. This will be proved in the experiment part of this paper. However, the inherent negative value still exists and cannot be ignored.

B. Passivation with Feed-forward Gain K

The physical mechanism of non-minimum phase is that it goes the opposite direction against the control signals. One of the efficient ways is to introduce a feed-forward compensation to enhance the input dynamics over the output. Based on this idea, the outer loop control block is modified as Fig. 5 shows.

Similarly, with the feed-forward compensation, the dynamic of outer loop plant is analyzed as follows.

$$G'_{vc} = K + G_{vc} \approx K + \alpha \frac{1 - s\beta}{1 + s\gamma} = \frac{(\alpha + K) - s(K\gamma - \alpha\beta)}{1 + s\gamma} \qquad (15)$$

where G'_{vc} is the equivalent plant with passive feed-forward compensation.

Replacing s with $j\omega$, the new plant becomes:

$$G'_{vc} \approx \frac{(\alpha + K) - s(K\gamma - \alpha\beta)}{1 + s\gamma}$$
$$= \frac{\alpha + K + \omega^2 \gamma (K\gamma - \alpha\beta) + j\omega [(K\gamma - \alpha\beta) - (\alpha + K)\gamma]}{1 + \omega^2 \gamma^2} \qquad (16)$$

Let ω goes to zero and positive infinite respectively, then the value at low frequency and high frequency asymptotic can be written as follows,

$$\omega \to 0, \quad G'_{vc} \to \alpha + K = \frac{D'R}{2R_f} + K \qquad (17)$$

$$\omega \to +\infty, \quad G'_{vc} \to K - \frac{\alpha\beta}{\gamma} = K - \frac{L}{R_f D'RC} \qquad (18)$$

If the feed-forward gain K equals to $\alpha\beta/\gamma$, the negative value can be compensated successfully, thus outer plant is positive real according to passive theory and the passivation process is completed.

However, it could be noticed that introducing the feed-forward gain K also alters the low frequency value from the equation (17). This will lead to the voltage reference droop and will further introduce voltage droop on the original quiescent operating point. The predicted compensated plant on s-plane is shown in Fig. 6.

In order to keep the original quiescent operating point unchanged, the quiescent operating point difference needs to be removed. Introducing the feed-forward compensation alters the dynamics at both low and high frequency, while the low
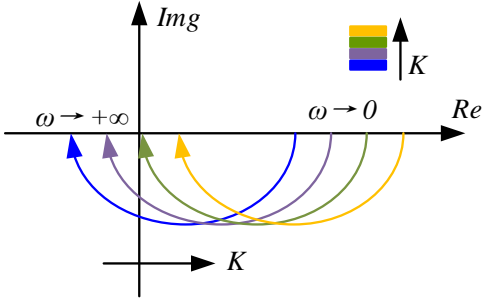
Fig. 6. Predicted locus of outer loop with passivation gain K on s-plane.

Fig. 7. Predicted locus of outer loop with passivation gain HPF-K on s-plane.

frequency alternation is not desired in most practical cases. Therefore, it should have a term to make the low frequency dynamic unchanged and compensate the high frequency negative value. Driven by this need, a high pass filter (HPF) has such feature is designed to meet the above requirement.

C. Passivation with Feed-forward HPF-K

Based on the requirements of suppressing the gain over low frequency to zero and keeping the high frequency part effective with gain K, a HPF is added to the feed-forward passive controller, which can be written as:

$$G_p = K \frac{s}{s + \delta} \quad (19)$$

where δ is the corner frequency of passive controller.

Similarly, the asymptotic values over low frequency and high frequency can be examined as follows,

$$G'_{vc} = \frac{sK}{s + \delta} + G_{vc} \approx \frac{\alpha (1 - s\beta)(s + \delta) + sK(1 + s\gamma)}{(s + \delta) \cdot (1 + s\gamma)} \quad (20)$$

Replacing s with $j\omega$, similarly, let ω goes to zero and positive infinite respectively, and check the values at low frequency and high frequency approximation,

$$\omega \to 0, \quad G'_{vc} \to \frac{\alpha \delta^2}{\delta^2} = \alpha = \frac{D'R}{2R_f} \quad (21)$$

$$\omega \to +\infty, \quad G'_{vc} \to \frac{-(\alpha\beta - K\gamma)\gamma\omega^4}{\gamma^2\omega^4} = K - \frac{L}{R_f D' RC} \quad (22)$$

It can be noticed from equation (21) and equation (22) that the low frequency dynamic is not altered, and high frequency dynamic is then compensated by introduced gain K as expected. The predicted compensated plant is drawn in Fig. 7. Therefore, the outer control loop is modified successfully from the above passive compensation as required.

IV. CONTROLLER DESIGN AND SIMULATION ANALYSIS

A. Controller Design

After the analysis of the passivation process described in Section III, the full control block diagram of the interface converter can be attained by appropriate manipulations, which is shown in Fig. 8. The block contains the following controllers:
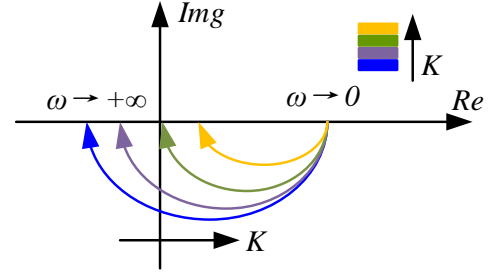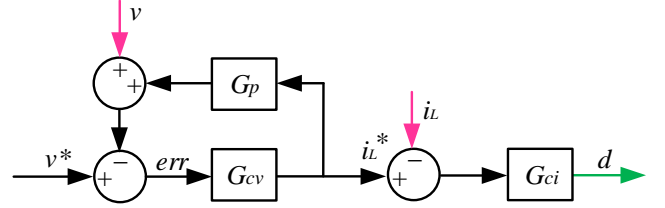

Fig. 8. Full control block diagram of boost converter integrated with passive controller.

$$G_{ci} = G_{im} \cdot \left(\frac{1 + \frac{2\pi f_{zi}}{s}}{1 + \frac{s}{2\pi f_{pi}}} \right) \quad (23)$$

$$G_{cv} = G_{vm} \cdot \left(1 + \frac{2\pi f_{zv}}{s} \right) \quad (24)$$

$$G_p = K \cdot \frac{s}{s + 2\pi f_p} \quad (25)$$

where G_{ci} is the inner loop controller; G_{cv} is the outer loop controller; and G_p is the passive controller.

The inner loop controller G_{ci} and outer loop controller G_{cv} can be designed from the conventional way with sufficient phase and magnitude margin. The proposed passive controller does not change the previous controllers and makes the whole system control complex. The only thing left now is how to design the passive controller G_p individually.

The feed-forward gain K is solved by the above analysis, which aims to compensate the negative value. Therefore, in practical it can be assigned with a value larger than the negative value. The corner frequency needs to be chosen from the frequency that outer loop plant enters the negative part in s-plane, which means it requires that f_p should satisfy the equation (26).

$$f_p < f_N \quad (26)$$

where f_N is the frequency that outer loop plant enters the negative part.

From the equation (12), the frequency that the plant steps into the negative area can be attained if let $1 - \omega^2 \beta\gamma = 0$. The frequency is then shown in equation (27).

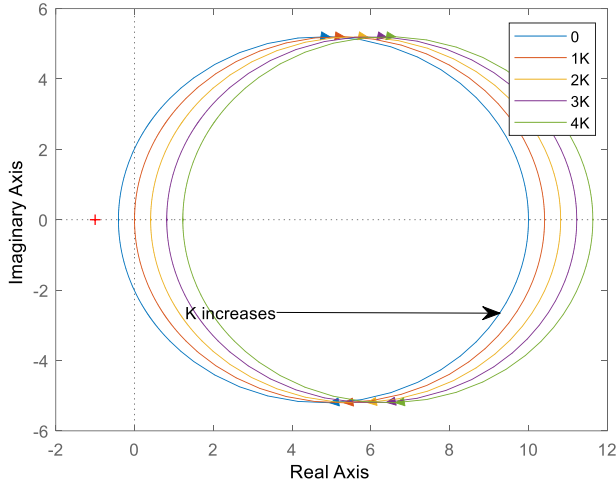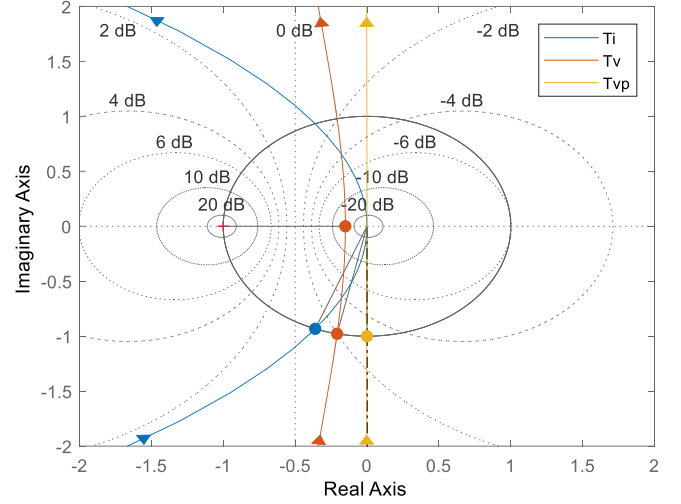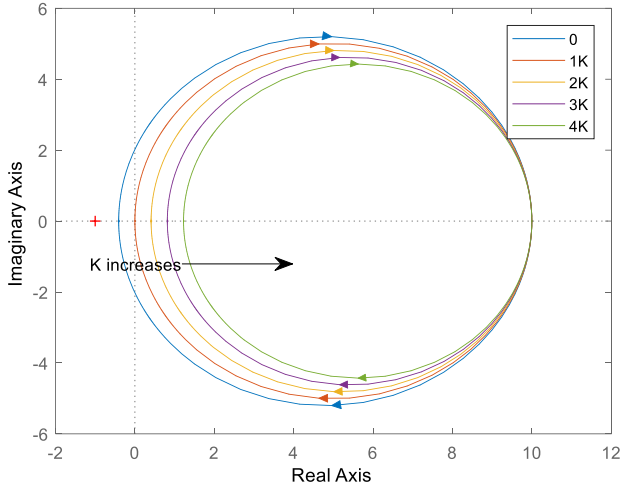$$f_N = \frac{1}{2\pi} \sqrt{\frac{1}{\beta\gamma}} \quad (27)$$

Fig. 9. Simulated locus of outer loop with passivation gain K.

Fig. 11. Closed loop margin test on the Nyquist diagram.

Fig. 10. Simulated locus of outer loop with passivation gain HPF-K.

Fig. 12. Applying droop control in the proposed controller for two paralleled converters.

Substituting equation (10) for β and γ in equation (27), the frequency entering negative area is written as,

$$f_N = \frac{1}{2\pi}\sqrt{\frac{2D'^2}{LC}} \tag{28}$$

Conducting the numerical analysis based on the parameters in Table I, the s-plane plots with passivation of K and HPF-K are shown in Fig. 9 and Fig. 10. The results are matched with the predicted results in Section III-B and Section III-C.

B. Impedance Analysis

Conventionally, margin test is used to evaluate the stability performance of designed controllers, e.g., in a Bode plot or Nyquist plot. The Nyquist plot of proposed passive controller is shown in Fig. 11. The inner current closed loop gain is T_i, and it can be observed that inner loop is stable and have sufficient phase margin. The outer voltage close loop gain is T_v, and with passive controller is T_{vp}. It can be seen that they

are stable; in addition, added feed-forward path provides more phase margin without changing previous voltage controller.

As droop control is usually applied in a DC microgrid, it is thus necessary to discuss if the proposed passive controller has negative impact on the output impedance. The droop control is implemented in the outside of double loop control, which is shown in Fig. 12. The voltage reference is modified by the output current and droop coefficient. From Fig. 2, the output admittance of this converter can be defined as:

$$Y_N = -\frac{\Delta i_o(s)}{\Delta v(s)}, N \in \{dbl, droop, passive, drpa\} \tag{29}$$

where Y_{dbl} is defined as output admittance with pure double loop controller; $Y_{passive}$ is defined as the output admittance with double loop controller and only with passive controller; Y_{droop} is defined as the output admittance with double loop controller and only with droop control; Y_{drpa} is defined as the output admittance with all controllers.

The small signal block of such output admittance is shown in Fig. 13. Two red-crosses are indicated in the figure for different admittance calculations. For example, to calculate $Y_{passive}$, the bottom R_v path can be deleted. The output admittance of converter shaped by passive controller is shown in Fig. 14.

Compared with conventional double loop control, it can be seen that the proposed passive controller decreases admittance in the low frequency band and flattens admittance in the high frequency band. In addition, the passive controller alters the phase angle over mid-high frequency and makes the converter
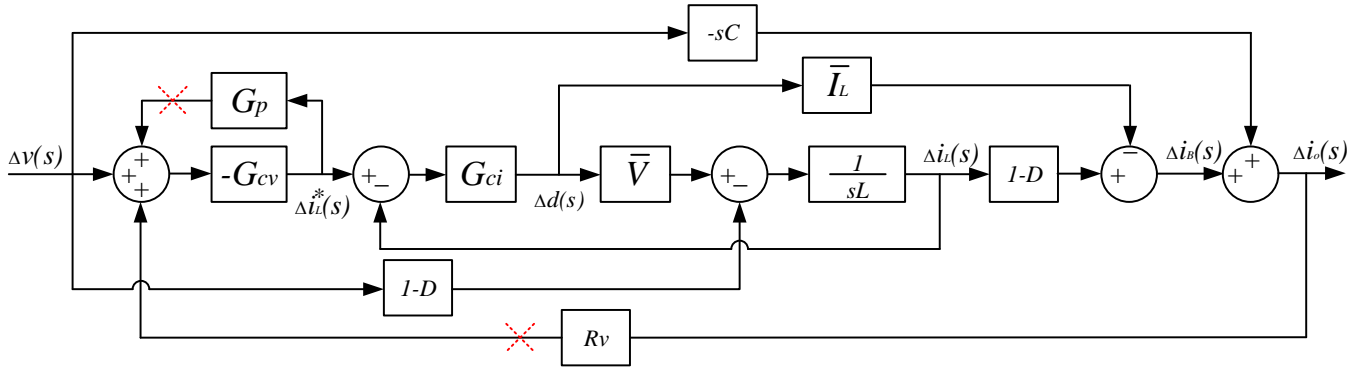
Fig. 13. Output admittance/impedance shaped by the passive controller.
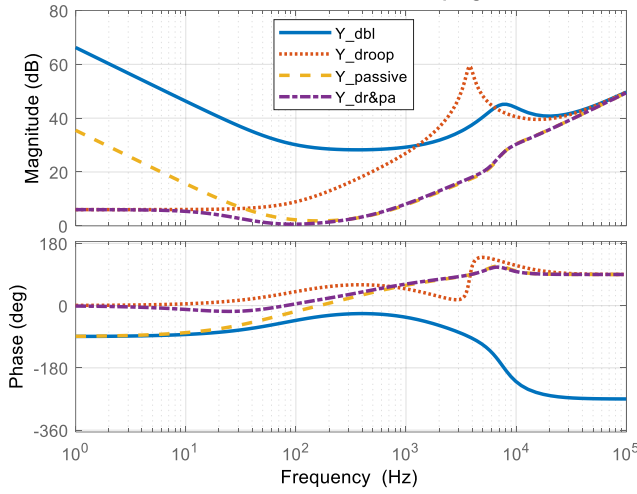
Fig. 14. Bode plot of Output admittance/impedance shaped by the passive controller.

Fig. 15. Impedance analysis of a DC microgrid.
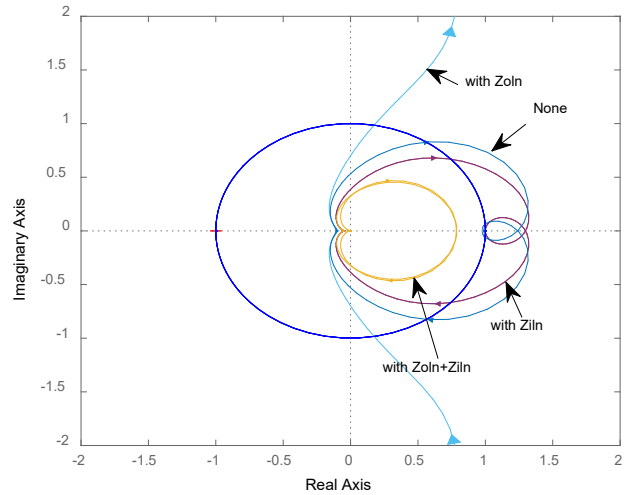
Fig. 16. Minor loop gain with constant power loads considering line impedance.

gain more capacitance. Similarly, droop control can alter the phase angle, and directly make the low frequency admittance to zero, which exhibits resistance and meet the expectations. The introduced passive controller does not change low frequency admittance and fattens the admittance over mid-high frequency. Therefore, the proposed control does not affect the stability performance of the original droop control for paralleled converters.

C. Cascaded with CPL

The analysis of the terminal impedance shaped by the proposed controller can be used to analyse the stability performance with CPL. CPL has negative incremental impedance, and this makes the system less damped and deteriorates the system stability. Such negative incremental impedance can be described as [26]:

$$\frac{\partial v_{bus}}{\partial i_{Load}} = \frac{\partial}{\partial i_{Load}}\left(\frac{P_L}{i_{Load}}\right) = -\frac{P_L}{i_{Load}^2} = -\frac{v_{bus}}{i_{Load}} \quad (30)$$

where P_L is the load power; i_{Load} is the load current; v_{bus} is the DC bus voltage.

The impedance distribution can be divided into two parts: the source-side output impedance and the load-side input impedance, labeled as $Z_o(s)$ and $Z_i(s)$ as shown in Fig. 15, respectively. In a DC microgrid, the total source-side and load-side impedance can be written in equation (31) and equation

(32), respectively.

$$Z_S = \left(\frac{1}{Z_1} + \frac{1}{Z_2} + \cdots + \frac{1}{Z_n} \right)^{-1} = \left(\sum_{o=1}^{n} \frac{1}{Z_o} \right)^{-1} \quad (31)$$

$$Z_L = \left(\frac{1}{Z_1} + \frac{1}{Z_2} + \cdots + \frac{1}{Z_m} \right)^{-1} = \left(\sum_{i=1}^{m} \frac{1}{Z_i} \right)^{-1} \quad (32)$$

where Z_S adn Z_L are the total source-side and load-side impedance; n and m are total number of source-side and load-side converters.

Considering the line impedance, either source-side or load-side impedance, the original impedance can be replaced by:

$$Z_o' = Z_o + Z_{oln} \quad (33)$$

$$Z_i' = Z_i + Z_{iln} \quad (34)$$

where Z_{oln} is the source-side line impedance and Z_{iln} is the load-side line impedance.

From conventional stability criteria [24], a minor loop gain (MLP) is defined to evaluate the stability performance of cascaded system.

$$T_{MLG} = \frac{Z_o}{Z_i} \quad (35)$$

Based on the above analysis, the minor loop gain by using the proposed control is shown in Fig. 16. Four curves can be seen in the figure. Without considering the line impedance, which is labeled with None in the figure, the MLP trace indicate the system stable. Similarly, considering line resistance on side or both sides in the case, the system is still stable. One interesting fact is that when only considering source-side line resistance (with Z_{oln} only), the system has the potential of being unstable as long as the line impedance is large enough. However, such issues can be solved by damped filter design [27], and such issue is out of scope of this paper. Therefore, it can be concluded that the cascaded system is stable in the proposed case study.

V. EXPERIMENTAL VALIDATION

The DC microgrid experimental test bench diagram is shown in Fig. 17. Two identical boost converters are used to connect the battery storage. The converter parameters applied in the section are based on the Table I. Several equivalent switches A, B, M, N and J are applied in the figure for illustration purpose. Switch A is a droop control switch. It is off when there is only one converter in the system. Switch B is a passive controller switch. It is used to validate the effectiveness of the proposed passive controller in the same operation condition. Switches M and N are used to choose different values of output capacitors. Switch J is for connecting/disconnecting another converter to the system.

The experimental validation has four parts. The first part is to validate the effectiveness of the proposed passivation method with feed-forward gain K for the interface converters. The second part is to validate that the modified feed-forward passive controller, which can stabilize the interface converter

TABLE I
PARAMETERS USED IN THE NUMERICAL AND EXPERIMENTAL ANALYSIS

Parameters	Values	Explanations
L	$240\mu H$	Inductor
C	$470\mu F$	Capacitor
R	10Ω	Load resistor
V_g	$25V$	Input source voltage
C	$470\mu F$	Output capacitor
V^*	$50V$	Reference voltage/nominal voltage
f_s	$25kHz$	Switching frequency
R_v	$0 - 2\Omega$	Virtual resistor
R_f	0.25	Current sampling gain
H	0.0075	Voltage sampling gain
G_{im}	0.3016	Inner loop current controller gain
G_{vm}	49.2183	Inner loop current controller gain
f_{zi}	$1kHz$	Inner loop current controller zero frequency
f_{pi}	$6.25kHz$	Inner loop current controller pole frequency
f_{zv}	$250Hz$	Outer loop voltage controller zero frequency
f_p	$50Hz$	Passive controller corner frequency
K	$0 - 2.5$	Passive controller gain
T_{sp}	$40\mu s$	Sampling period
Z_{iln}	$0.5\Omega + 10\mu H$	Load-side input line impedance
Z_{oln}	$0.5\Omega + 10\mu H$	Source-side output line impedance

Fig. 17. Experimental test configurations.

without changing the original quiescent operating point. In these two cases, Switch A is off. The third part is two paralleled boost converters operate in the DC microgrid where switches A, B and J are on. Finally, a practical DC microgrid operation is enabled with PV source shown in the Fig. 17. It is switched on to emulate dynamic source power fluctuations.

A. Validation of Passive Controllers

It can be seen from equation (14) that reducing the output capacitor or increasing the load power will tend to make the system less stable. To demonstrate this, the value of the output capacitor is reduced from $470\mu F$ to $100\mu F$ through switches
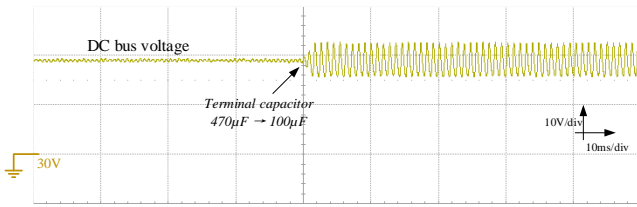
Fig. 18. Reducing the terminal capacitor to make the system oscillate.

Fig. 19. Unstable case becomes stable by applying passive control with expected voltage drop.

Fig. 20. Unstable case becomes stable by applying passive control with HPF, K=1.9.

Fig. 21. Unstable case becomes stable by applying passive control with HPF, K=2.5.

Fig. 22. Instability occurs when the passivation controller is removed from two parallel interface converters with average current sharing droop control.

M and N. The experimental results (Fig. 18) show that once the capacitor is switched to $100\mu F$, the oscillation occurs as predicted. This shows the closed loop controller can not compensate the NMP effect.

When the feed-forward compensator of gain K is switched on, the oscillation is then disappeared as the result shown in Fig. 19. An obvious voltage drop occurs because the introduced feed-forward gain K impact the quiescent operating point as predicted. Therefore, it can be concluded that the proposed passive controller can effectively compensate the NMP effect.

B. Modified Passive Controllers

The second part is to show the effectiveness of feed-forward compensator with a high pass filter. In most practical applications, the natural voltage droop caused by the feed-forward gain K is not desired, and it is better to keep the original features of the converter. Therefore, the high pass filter shows importance in this situation. The passivation results are shown in Fig. 20 and Fig. 21. It can be seen from Fig. 21 that sufficient feed-forward gain has better performance while the less compensated gain still has minor oscillation even though original oscillation has been greatly suppressed. This is because the plant transfer function of the less compensated case may still traverse into the left plane on the s-plane. As predicted, the introduced high pass filter will eliminate the impact on the alteration of quiescent operating point.

C. Droop Controlled Converters in a DC Microgrid

In this test, another boost converter is switched on through switch J and the instability can occur in two paralleled interface converters. Two interface converters are both working at droop control with average current sharing. Once the passive controllers are switched off, the instability occurs immediately, which is shown in Fig. 22.
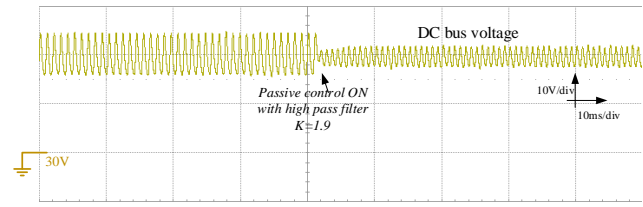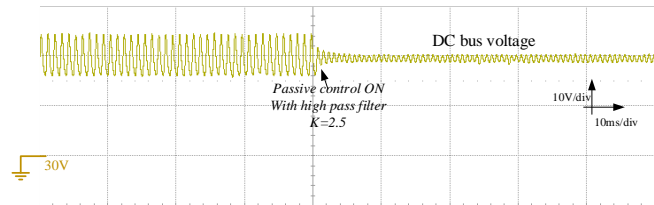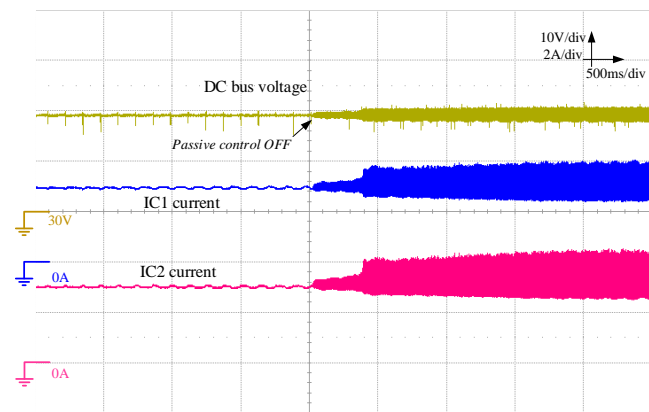
Therefore, the effectiveness of the proposed passive controller is experimentally validated. Adding the passivation loop can improve the stability of boost converters. It can help to enhance the stable performance in dealing with the fast and frequent load variations and load power sharing in the DC microgrid. The feed-forward gain is also adjustable and easy to be tuned by the engineers.

D. Practical DC Microgrid Operations

In a practical DC microgrid, the DC bus voltage could fluctuate due to the secondary control methods, such as DC bus signalling method. In those scenarios, the frequent DC bus voltage variations proposes a challenge to the primary control. With the proposed primary passive control, the system can always be stable, as shown in the experimental result Fig. 23. In this experiment, the system feeds an electronic load under CPL mode and a resistor. The programmable electronics load steps up and down under a testing mode. Meanwhile, the
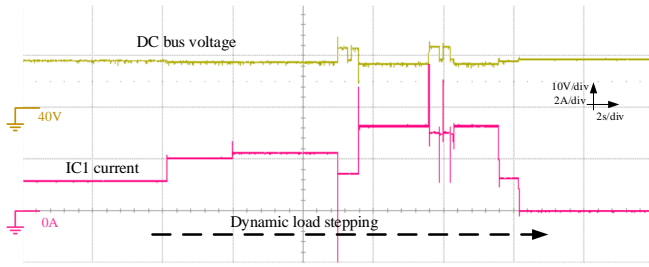
Fig. 23. Practical DC microgrid operation test with load and voltage disturbance.
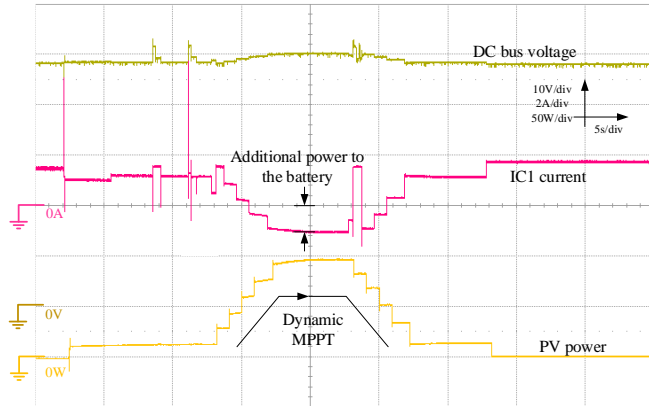

Fig. 24. Practical DC microgrid operation test with source and voltage disturbance.

DC bus voltage reference actively changes during the load variation to test the robustness of the proposed controller.

Apart from load variations test, the input source variation is also conducted. The PV power varies between 0W and 100W, and the experimental result is shown in Fig. 24. It shows the frequent DC bus voltage variations and PV source fluctuations will not affect the system stability.

VI. CONCLUSIONS

This paper presents a novel passive controller design for boost converters to deal with instability caused by the NMP effect. The passive theory and how this theory can be applied to the controller design are briefly introduced. The proposed passive controller makes the system transfer function react positive realness such that simplifies the control design and gain more controllability and stability. Two types of controller are introduced and discussed: feed-forward passive gain K and feed-forward passive controller HPF-K. Both of them are experimentally validated and the experimental results match the theoretical and numerical analysis.
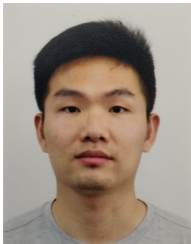
REFERENCES

[1] X. Zhao, Y. W. Li, H. Tian, and X. Wu, "Energy management strategy of multiple supercapacitors in a dc microgrid using adaptive virtual impedance," *IEEE Journal of Emerging and Selected Topics in Power Electronics*, vol. 4, no. 4, pp. 1174–1185, 2016.

[2] Wei-Chung Wu, R. M. Bass, and J. R. Yeargan, "Eliminating the effects of the right-half plane zero in fixed frequency boost converters," in *PESC 98 Record. 29th Annual IEEE Power Electronics Specialists Conference*, vol. 1, May 1998, pp. 362–366 vol.1.

[3] Y. Gu, W. Li, and X. He, "Passivity-based control of dc microgrid for self-disciplined stabilization," *IEEE Transactions on Power Systems*, vol. 30, no. 5, pp. 2623–2632, 2015.

[4] F. Chen, R. Burgos, D. Boroyevich, J. C. Vasquez, and J. M. Guerrero, "Investigation of nonlinear droop control in dc power distribution systems: Load sharing, voltage regulation, efficiency, and stability," *IEEE Transactions on Power Electronics*, vol. 34, no. 10, pp. 9404–9421, 2019.

[5] J. Calvente, L. Martinez-Salamero, H. Valderrama, and E. Vidal-Idiarte, "Using magnetic coupling to eliminate right half-plane zeros in boost converters," *IEEE Power Electronics Letters*, vol. 2, no. 2, pp. 58–62, June 2004.

[6] Y. Luo, Y. Su, Y. Huang, Y. Lee, K. Chen, and W. Hsu, "Time-multiplexing current balance interleaved current-mode boost dc-dc converter for alleviating the effects of right-half-plane zero," *IEEE Transactions on Power Electronics*, vol. 27, no. 9, pp. 4098–4112, Sep. 2012.

[7] S. Kolluri and L. N. Narasamma, "A new auxiliary current injection circuit for improved transient response of step-up/step-down dc-dc converters," in *IECON 2013 - 39th Annual Conference of the IEEE Industrial Electronics Society*, Nov 2013, pp. 216–221.

[8] B. Poorali and E. Adib, "Right-half-plane zero elimination of boost converter using magnetic coupling with forward energy transfer," *IEEE Transactions on Industrial Electronics*, vol. 66, no. 11, pp. 8454–8462, Nov 2019.

[9] K. Viswanathan, R. Oruganti, and D. Srinivasan, "A novel tri-state boost converter with fast dynamics," *IEEE Transactions on Power Electronics*, vol. 17, no. 5, pp. 677–683, Sep. 2002.

[10] D. M. Sable, B. H. Cho, and R. B. Ridley, "Use of leading-edge modulation to transform boost and flyback converters into minimum-phase-zero systems," *IEEE Transactions on Power Electronics*, vol. 6, no. 4, pp. 704–711, Oct 1991.

[11] D. M. Sable, B. H. Cho, and R. B. Ridley, "Elimination of the positive zero in fixed frequency boost and flyback converters," in *Fifth Annual Proceedings on Applied Power Electronics Conference and Exposition*, 1990, pp. 205–211.

[12] V. V. Paduvalli, R. J. Taylor, L. R. Hunt, and P. T. Balsara, "Mitigation of positive zero effect on nonminimum phase boost dc/dc converters in ccm," *IEEE Transactions on Industrial Electronics*, vol. 65, no. 5, pp. 4125–4134, May 2018.

[13] Y. M. Roshan and M. Moallem, "Control of nonminimum phase load current in a boost converter using output redefinition," *IEEE Transactions on Power Electronics*, vol. 29, no. 9, pp. 5054–5062, Sep. 2014.

[14] Y. I. Son and I. H. Kim, "Complementary pid controller to passivity-based nonlinear control of boost converters with inductor resistance," *IEEE Transactions on Control Systems Technology*, vol. 20, no. 3, pp. 826–834, May 2012.

[15] T. Kobaku, S. C. Patwardhan, and V. Agarwal, "Experimental evaluation of internal model control scheme on a dc/dc boost converter exhibiting nonminimum phase behavior," *IEEE Transactions on Power Electronics*, vol. 32, no. 11, pp. 8880–8891, Nov 2017.

[16] R. W. Erickson and D. Maksimović, *Fundamentals of Power Electronics*, 2nd ed. Boston, MA: Springer US, 2001, ch. 12, pp. 439–487.

[17] M. A. Hassan, E. Li, X. Li, T. Li, C. Duan, and S. Chi, "Adaptive passivity-based control of dc-dc buck power converter with constant power load in dc microgrid systems," *IEEE Journal of Emerging and Selected Topics in Power Electronics*, vol. 7, no. 3, pp. 2029–2040, 2019.

[18] M. Cucuzzella, R. Lazzari, Y. Kawano, K. C. Kosaraju, and J. M. A. Scherpen, "Robust passivity-based control of boost converters in dc microgrids," in *2019 IEEE 58th Conference on Decision and Control (CDC)*, 2019, pp. 8435–8440.

[19] K. C. Kosaraju, M. Cucuzzella, J. M. A. Scherpen, and R. Pasumarthy, "Differentiation and passivity for control of brayton-moser systems," *IEEE Transactions on Automatic Control*, pp. 1–1, 2020.

[20] J. Zeng, Z. Zhang, and W. Qiao, "An interconnection and damping assignment passivity-based controller for a dc-dc boost converter with a constant power load," *IEEE Transactions on Industry Applications*, vol. 50, no. 4, pp. 2314–2322, 2014.

[21] C. M. Wildrick, F. C. Lee, B. H. Cho, and B. Choi, "A method of defining the load impedance specification for a stable distributed power system," *IEEE Transactions on Power Electronics*, vol. 10, no. 3, pp. 280–285, 1995.

[22] A. M. Rahimi and A. Emadi, "Active damping in dc/dc power electronic converters: A novel method to overcome the problems of constant power loads," *IEEE Transactions on Industrial Electronics*, vol. 56, no. 5, pp. 1428–1439, 2009.

[23] A. Riccobono and E. Santi, "A novel passivity-based stability criterion (pbsc) for switching converter dc distribution systems," in *2012 Twenty-*
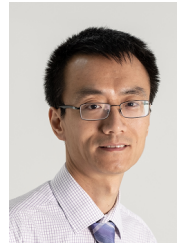
Seventh Annual IEEE Applied Power Electronics Conference and Exposition (APEC), 2012, pp. 2560–2567.

[24] A. Riccobono and E. Santi, "Comprehensive review of stability criteria for dc power distribution systems," *IEEE Transactions on Industry Applications*, vol. 50, no. 5, pp. 3525–3535, 2014.

[25] J. Bao and P. L. Lee, *Process Control: The Passive Systems Approach*, 1st ed. London: Springer London, 2007, ch. 2, pp. 5–41.

[26] X. Lu, K. Sun, J. M. Guerrero, J. C. Vasquez, L. Huang, and J. Wang, "Stability enhancement based on virtual impedance for dc microgrids with constant power loads," *IEEE Transactions on Smart Grid*, vol. 6, no. 6, pp. 2770–2783, 2015.

[27] M. Cespedes, L. Xing, and J. Sun, "Constant-power load system stabilization by passive damping," *IEEE Transactions on Power Electronics*, vol. 26, no. 7, pp. 1832–1836, 2011.

Zhengyu Lin (S'03âM'05âSM'10) received the B.Sc. and M.Sc. degrees from the College of Electrical Engineering, Zhejiang University, Hangzhou, China, in 1998 and 2001, respectively, and the Ph.D. degree from Herio-Watt University, Edinburgh, U.K., in 2005. He is currently a Senior Lecturer in the School of Mechanical, Electrical and Manufacturing Engineering, Loughborough University, Loughborough, UK.

His research interests include power electronics and its applications in renewable energy, energy storage, motor drives, microgrids, and multi-energy systems. He is currently holding an EPSRC UKRI Innovation Fellowship on DC microgrids.

Fulong Li (S'16-M'20) received the B.S. degree in electrical engineering from Yangzhou University, Yangzhou, China, in 2015, and Ph.D. from Aston University, Birmingham, UK, in 2019. He is currently a Research Associate in Loughborough University, U.K.

His current research interests include control and stability analysis of power electronics converters applied in DC microgrids and distributed power systems, and energy management system design of microgrids.